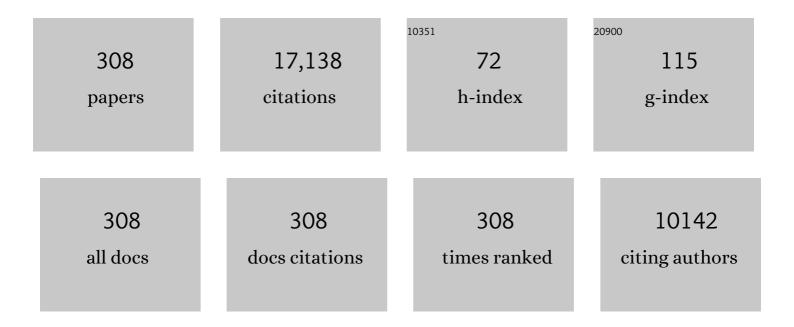
## Masoud Salavati-Niasari

List of Publications by Year in descending order

Source: https://exaly.com/author-pdf/5916067/publications.pdf Version: 2024-02-01



#	Article	IF	CITATIONS
1	Synthesis, characterization and application of Co/Co3O4 nanocomposites as an effective photocatalyst for discoloration of organic dye contaminants in wastewater and antibacterial properties. Journal of Molecular Liquids, 2021, 337, 116405.	2.3	553
2	Control sonochemical parameter to prepare pure Zn0.35Fe2.65O4 nanostructures and study their photocatalytic activity. Ultrasonics Sonochemistry, 2019, 58, 104619.	3.8	376
3	Dy <sub>2</sub> BaCuO <sub>5</sub> /Ba <sub>4</sub> DyCu <sub>3</sub> O <sub>9.09</sub> Sâ€scheme heterojunction nanocomposite with enhanced photocatalytic and antibacterial activities. Journal of the American Ceramic Society, 2021, 104, 2952-2965.	1.9	370
4	Green sonochemical synthesis of BaDy <sub>2</sub> NiO <sub>5</sub> /Dy <sub>2</sub> O <sub>3</sub> and BaDy <sub>2</sub> NiO <sub>5</sub> /NiO nanocomposites in the presence of core almond as a capping agent and their application as photocatalysts for the removal of organic dyes in water. RSC Advances, 2021, 11, 11500-11512.	1.7	346
5	Eco-friendly synthesis of Nd2Sn2O7–based nanostructure materials using grape juice as green fuel as photocatalyst for the degradation of erythrosine. Composites Part B: Engineering, 2019, 167, 643-653.	5.9	312
6	Photo-degradation of organic dyes: simple chemical synthesis of Ni(OH)2 nanoparticles, Ni/Ni(OH)2 and Ni/NiO magnetic nanocomposites. Journal of Materials Science: Materials in Electronics, 2016, 27, 1244-1253.	1.1	295
7	Facile fabrication of silver iodide/graphitic carbon nitride nanocomposites by notable photo-catalytic performance through sunlight and antimicrobial activity. Journal of Hazardous Materials, 2020, 389, 122079.	6.5	268
8	Hydrothermal green synthesis of magnetic Fe3O4-carbon dots by lemon and grape fruit extracts and as a photoluminescence sensor for detecting of E. coli bacteria. Spectrochimica Acta - Part A: Molecular and Biomolecular Spectroscopy, 2018, 203, 481-493.	2.0	217
9	Green synthesis of dysprosium stannate nanoparticles using Ficus carica extract as photocatalyst for the degradation of organic pollutants under visible irradiation. Ceramics International, 2020, 46, 6095-6107.	2.3	212
10	Nd2Sn2O7 nanostructures: Green synthesis and characterization using date palm extract, a potential electrochemical hydrogen storage material. Ceramics International, 2020, 46, 17186-17196.	2.3	199
11	Fabrication and characterization of Fe 3 O 4 @SiO 2 @TiO 2 @Ho nanostructures as a novel and highly efficient photocatalyst for degradation of organic pollution. Journal of Energy Chemistry, 2017, 26, 17-23.	7.1	196
12	Grafting of CuFe12O19 nanoparticles on CNT and graphene: Eco-friendly synthesis, characterization and photocatalytic activity. Journal of Cleaner Production, 2018, 176, 1185-1197.	4.6	193
13	Tl <sub>4</sub> Cdl <sub>6</sub> Nanostructures: Facile Sonochemical Synthesis and Photocatalytic Activity for Removal of Organic Dyes. Inorganic Chemistry, 2018, 57, 11443-11455.	1.9	179
14	Electrochemical hydrogen storage capacity and optical properties of NiAl2O4/NiO nanocomposite synthesized by green method. International Journal of Hydrogen Energy, 2017, 42, 5235-5245.	3.8	176
15	Simple sol-gel synthesis and characterization of new CoTiO3/CoFe2O4 nanocomposite by using liquid glucose, maltose and starch as fuel, capping and reducing agents. Journal of Colloid and Interface Science, 2018, 514, 723-732.	5.0	176
16	A sonochemical method for synthesis of Fe3O4 nanoparticles and thermal stable PVA-based magnetic nanocomposite. Journal of Industrial and Engineering Chemistry, 2014, 20, 3970-3974.	2.9	174
17	Caffeine: A novel green precursor for synthesis of magnetic CoFe2O4 nanoparticles and pH-sensitive magnetic alginate beads for drug delivery. Materials Science and Engineering C, 2017, 76, 1085-1093.	3.8	174
18	Nd2O3-SiO2 nanocomposites: A simple sonochemical preparation, characterization and photocatalytic activity. Ultrasonics Sonochemistry, 2018, 42, 171-182.	3.8	174

#	Article	IF	CITATIONS
19	Degradation of methylene blue and Rhodamine B as water pollutants via green synthesized Co3O4/ZnO nanocomposite. Journal of Molecular Liquids, 2017, 229, 293-299.	2.3	169
20	Electro-spinning of cellulose acetate nanofibers/Fe/carbon dot as photoluminescence sensor for mercury (II) and lead (II) ions. Carbohydrate Polymers, 2020, 229, 115428.	5.1	168
21	Recyclable magnetic superhydrophobic straw soot sponge for highly efficient oil/water separation. Journal of Colloid and Interface Science, 2017, 497, 57-65.	5.0	166
22	Photoluminescence carbon dot as a sensor for detecting of Pseudomonas aeruginosa bacteria: Hydrothermal synthesis of magnetic hollow NiFe2O4-carbon dots nanocomposite material. Composites Part B: Engineering, 2019, 161, 564-577.	5.9	164
23	Enhanced photodegradation of dye in waste water using iron vanadate nanocomposite; ultrasound-assisted preparation and characterization. Ultrasonics Sonochemistry, 2017, 39, 494-503.	3.8	163
24	Novel synthesis of Zn2GeO4/graphene nanocomposite for enhanced electrochemical hydrogen storage performance. International Journal of Hydrogen Energy, 2017, 42, 17184-17191.	3.8	161
25	Magnetically retrievable ferrite nanoparticles in the catalysis application. Advances in Colloid and Interface Science, 2019, 271, 101982.	7.0	161
26	A simple sonochemical approach for synthesis and characterization of Zn2SiO4 nanostructures. Ultrasonics Sonochemistry, 2016, 29, 226-235.	3.8	158
27	Microwave-assisted synthesis and photovoltaic measurements of CuInS2 nanoparticles prepared by using metal–organic precursors. Materials Research Bulletin, 2012, 47, 3148-3159.	2.7	157
28	Self-assembly of hydrogen storage materials based multi-walled carbon nanotubes (MWCNTs) and Dy3Fe5O12 (DFO) nanoparticles. Journal of Alloys and Compounds, 2018, 745, 789-797.	2.8	157
29	Application of ultrasound-aided method for the synthesis of NdVO4 nano-photocatalyst and investigation of eliminate dye in contaminant water. Ultrasonics Sonochemistry, 2018, 42, 201-211.	3.8	156
30	Design of Magnetically Recyclable Ternary Fe <sub>2</sub> O <sub>3</sub> /EuVO <sub>4</sub> /g-C <sub>3</sub> N <sub>4</sub> Nanocomposites for Photocatalytic and Electrochemical Hydrogen Storage. ACS Applied Energy Materials, 2021, 4, 680-695.	2.5	156
31	Synthesis and adsorption studies of NiO nanoparticles in the presence of H2acacen ligand, for removing Rhodamine B in wastewater treatment. Chemical Engineering Research and Design, 2015, 93, 282-292.	2.7	153
32	Green synthesis of magnetic chitosan nanocomposites by a new sol–gel auto-combustion method. Journal of Magnetism and Magnetic Materials, 2016, 410, 27-33.	1.0	150
33	Enhanced visible-light-driven photocatalytic performance for degradation of organic contaminants using PbWO4 nanostructure fabricated by a new, simple and green sonochemical approach. Ultrasonics Sonochemistry, 2021, 72, 105420.	3.8	149
34	Nanoscale microreactor-encapsulation of 18-membered decaaza macrocycle nickel(II) complexes. Inorganic Chemistry Communication, 2005, 8, 174-177.	1.8	148
35	Silver chromate and silver dichromate nanostructures: Sonochemical synthesis, characterization, and photocatalytic properties. Materials Research Bulletin, 2013, 48, 2084-2094.	2.7	146
36	Nd2Zr2O7-Nd2O3 nanocomposites: New facile synthesis, characterization and investigation of photocatalytic behaviour. Materials Letters, 2016, 180, 27-30.	1.3	144

#	Article	IF	CITATIONS
37	Synthesis and Characterization of Host (Nanodimensional Pores of Zeolite-Y)–Guest [Unsaturated 16-Membered Octaaza–macrocycle Manganese(II), Cobalt(II), Nickel(II), Copper(II), and Zinc(II) Complexes] Nanocomposite Materials. Chemistry Letters, 2005, 34, 1444-1445.	0.7	143
38	Freeze-drying synthesis, characterization and in vitro bioactivity of chitosan/graphene oxide/hydroxyapatite nanocomposite. RSC Advances, 2014, 4, 25993.	1.7	143
39	Nanodimensional Microreactor-encapsulation of 18-Membered Decaaza Macrocycle Copper(II) Complexes. Chemistry Letters, 2005, 34, 244-245.	0.7	142
40	Long chain polymer assisted synthesis of flower-like cadmium sulfide nanorods via hydrothermal process. Journal of Alloys and Compounds, 2009, 481, 776-780.	2.8	140
41	Investigation of the electrochemical hydrogen storage and photocatalytic properties of CoAl2O4 pigment: Green synthesis and characterization. International Journal of Hydrogen Energy, 2016, 41, 9418-9426.	3.8	139
42	Synthesis and characterization of spherical silica nanoparticles by modified Stöber process assisted by organic ligand. Superlattices and Microstructures, 2013, 61, 33-41.	1.4	138
43	Nanoscale microreactor-encapsulation 14-membered nickel(II) hexamethyl tetraaza: synthesis, characterization and catalytic activity. Journal of Molecular Catalysis A, 2005, 229, 159-164.	4.8	136
44	Gd2ZnMnO6/ZnO nanocomposites: Green sol-gel auto-combustion synthesis, characterization and photocatalytic degradation of different dye pollutants in water. Journal of Alloys and Compounds, 2020, 835, 155240.	2.8	135
45	Modified single-phase hematite nanoparticles via a facile approach for large-scale synthesis. Chemical Engineering Journal, 2011, 170, 278-285.	6.6	133
46	Synthesis of star-shaped PbS nanocrystals using single-source precursor. Journal of Alloys and Compounds, 2010, 507, 77-83.	2.8	132
47	Green synthesis using cherry and orange juice and characterization of TbFeO3 ceramic nanostructures and their application as photocatalysts under UV light for removal of organic dyes in water. Journal of Cleaner Production, 2020, 252, 119765.	4.6	132
48	ZnO nanotriangles: Synthesis, characterization and optical properties. Journal of Alloys and Compounds, 2009, 476, 908-912.	2.8	131
49	Star-shaped PbS nanocrystals prepared by hydrothermal process in the presence of thioglycolic acid. Polyhedron, 2012, 35, 149-153.	1.0	127
50	Synthesis and characterization of NiO nanoclusters via thermal decomposition. Polyhedron, 2009, 28, 1111-1114.	1.0	122
51	Simple sonochemical synthesis and characterization of HgSe nanoparticles. Ultrasonics Sonochemistry, 2012, 19, 1079-1086.	3.8	117
52	Facile microwave synthesis, characterization, and solar cell application of selenium nanoparticles. Journal of Alloys and Compounds, 2014, 617, 627-632.	2.8	113
53	Enhanced photocatalytic degradation of toxic contaminants using Dy2O3-SiO2 ceramic nanostructured materials fabricated by a new, simple and rapid sonochemical approach. Ultrasonics Sonochemistry, 2022, 82, 105892.	3.8	108
54	Preparation of PbO nanocrystals via decomposition of lead oxalate. Polyhedron, 2009, 28, 2263-2267.	1.0	107

#	Article	IF	CITATIONS
55	Simple fabrication of Pr2Ce2O7 nanostructures via a new and eco-friendly route; a potential electrochemical hydrogen storage material. Journal of Alloys and Compounds, 2019, 791, 792-799.	2.8	107
56	Passivation Mechanism Exploiting Surface Dipoles Affords High-Performance Perovskite Solar Cells. Journal of the American Chemical Society, 2020, 142, 11428-11433.	6.6	107
57	The inhibition of mild steel corrosion in hydrochloric acid media by two Schiff base compounds. Journal of Materials Science, 2009, 44, 2444-2453.	1.7	102
58	Size controllable synthesis of cobalt vanadate nanostructures with enhanced photocatalytic activity for the degradation of organic dyes. Journal of Molecular Catalysis A, 2016, 425, 31-42.	4.8	97
59	Facile synthesis, characterization and magnetic property of CuFe 12 O 19 nanostructures via a sol–gel auto-combustion process. Journal of Magnetism and Magnetic Materials, 2016, 401, 362-369.	1.0	92
60	PbTiO3/PbFe12O19 nanocomposites: Green synthesis through an eco-friendly approach. Composites Part B: Engineering, 2016, 85, 170-175.	5.9	90
61	Enhanced antibacterial activity and photocatalytic degradation of organic dyes under visible light using cesium lead iodide perovskite nanostructures prepared by hydrothermal method. Separation and Purification Technology, 2020, 253, 117526.	3.9	89
62	In vitro comparative study of pure hydroxyapatite nanorods and novel polyethylene glycol/graphene oxide/hydroxyapatite nanocomposite. Journal of Nanoparticle Research, 2014, 16, 1.	0.8	88
63	Simple and eco-friendly synthesis of recoverable zinc cobalt oxide-based ceramic nanostructure as high-performance photocatalyst for enhanced photocatalytic removal of organic contamination under solar light. Separation and Purification Technology, 2021, 267, 118667.	3.9	87
64	Facile precipitation synthesis and electrochemical evaluation of Zn2SnO4 nanostructure as a hydrogen storage material. International Journal of Hydrogen Energy, 2017, 42, 12420-12429.	3.8	85
65	Effect of Li <sub>2</sub> CoMn <sub>3</sub> O <sub>8</sub> Nanostructures Synthesized by a Combustion Method on Montmorillonite K10 as a Potential Hydrogen Storage Material. Journal of Physical Chemistry C, 2018, 122, 16498-16509.	1.5	84
66	Hydroxyapatite nanocrystals: Simple preparation, characterization and formation mechanism. Materials Science and Engineering C, 2014, 45, 29-36.	3.8	83
67	Effects of copper:aluminum ratio in CuO/Al 2 O 3 nanocomposite: Electrochemical hydrogen storage capacity, band gap and morphology. International Journal of Hydrogen Energy, 2016, 41, 15141-15148.	3.8	81
68	Sol–gel auto-combustion synthesis of PbFe <sub>12</sub> O <sub>19</sub> using maltose as a novel reductant. RSC Advances, 2014, 4, 63946-63950.	1.7	80
69	Facile synthesis, characterization and optical properties of copper vanadate nanostructures for enhanced photocatalytic activity. Journal of Materials Science: Materials in Electronics, 2016, 27, 4871-4878.	1.1	80
70	Novel Schiff base ligand-assisted in-situ synthesis of Cu3V2O8 nanoparticles via a simple precipitation approach. Journal of Molecular Liquids, 2016, 216, 59-66.	2.3	80
71	Fabrication of nanocomposite photocatalyst CuBi2O4/Bi3ClO4 for removal of acid brown 14 as water pollutant under visible light irradiation. Journal of Hazardous Materials, 2019, 361, 210-220.	6.5	80
72	Copper iodide decorated graphitic carbon nitride sheets with enhanced visible-light response for photocatalytic organic pollutant removal and antibacterial activities. Ecotoxicology and Environmental Safety, 2021, 208, 111712.	2.9	77

#	Article	IF	CITATIONS
73	Enhancement of magnetic, electrochemical and photocatalytic properties of lead hexaferrites with coating graphene and CNT: Sol-gel auto-combustion synthesis by valine. Separation and Purification Technology, 2017, 185, 140-148.	3.9	75
74	Amino acid assisted-synthesis and characterization of magnetically retrievable ZnCo2O4–Co3O4 nanostructures as high activity visible-light-driven photocatalyst. International Journal of Hydrogen Energy, 2020, 45, 22761-22774.	3.8	74
75	Simple morphology-controlled fabrication of nickel chromite nanostructures via a novel route. Chemical Engineering Journal, 2015, 279, 605-614.	6.6	73
76	NiTiO3/NiFe2O4 nanocomposites: Simple sol–gel auto-combustion synthesis and characterization by utilizing onion extract as a novel fuel and green capping agent. Materials Science in Semiconductor Processing, 2016, 43, 34-40.	1.9	73
77	Simple synthesis-controlled fabrication of thallium cadmium iodide nanostructures via a novel route and photocatalytic investigation in degradation of toxic dyes. Inorganica Chimica Acta, 2017, 455, 88-97.	1.2	73
78	Simple approach for the synthesis of Dy2Sn2O7 nanostructures as a hydrogen storage material from banana juice. Journal of Cleaner Production, 2019, 222, 103-110.	4.6	73
79	Transition metal selenides and diselenides: Hydrothermal fabrication, investigation of morphology, particle size and and their applications in photocatalyst. Advances in Colloid and Interface Science, 2021, 287, 102321.	7.0	72
80	Preparation, characterization and photocatalytic properties of Ag2Znl4/AgI nanocomposites via a new simple hydrothermal approach. Journal of Molecular Liquids, 2017, 225, 645-651.	2.3	71
81	Hydrothermal architecture of Cu5V2O10 nanostructures as new electro-sensing catalysts for voltammetric quantification of mefenamic acid in pharmaceuticals and biological samples. Biosensors and Bioelectronics, 2021, 178, 113017.	5.3	71
82	Green synthesis and characterization of RGO/Cu nanocomposites as photocatalytic degradation of organic pollutants in waste-water. International Journal of Hydrogen Energy, 2021, 46, 20534-20546.	3.8	71
83	Synthesis and characterization of a nickel selenide series via a hydrothermal process. Superlattices and Microstructures, 2014, 65, 79-90.	1.4	69
84	Synthesis, characterization and degradation of organic dye over Co <sub>3</sub> O <sub>4</sub> nanoparticles prepared from new binuclear complex precursors. RSC Advances, 2014, 4, 46517-46520.	1.7	68
85	Electrochemical sensor based on a chitosan-molybdenum vanadate nanocomposite for detection of hydroxychloroquine in biological samples. Journal of Colloid and Interface Science, 2022, 613, 1-14.	5.0	68
86	Magnetic Lu <sub>2</sub> Cu <sub>2</sub> O <sub>5</sub> -based ceramic nanostructured materials fabricated by a simple and green approach for an effective photocatalytic degradation of organic contamination. RSC Advances, 2021, 11, 40100-40111.	1.7	68
87	Utilizing maleic acid as a novel fuel for synthesis of PbFe12O19 nanoceramics via sol–gel auto-combustion route. Materials Characterization, 2015, 103, 11-17.	1.9	66
88	Physicochemical Interface Engineering of Cul/Cu as Advanced Potential Hole-Transporting Materials/Metal Contact Couples in Hysteresis-Free Ultralow-Cost and Large-Area Perovskite Solar Cells. Journal of Physical Chemistry C, 2017, 121, 21935-21944.	1.5	65
89	Sonochemical synthesis, characterization and application of PrVO4 nanostructures as an effective photocatalyst for discoloration of organic dye contaminants in wastewater. Ultrasonics Sonochemistry, 2020, 61, 104822.	3.8	65
90	Sonochemical synthesis of Dy2(CO3)3 nanoparticles, Dy(OH)3 nanotubes and their conversion to Dy2O3 nanoparticles. Ultrasonics Sonochemistry, 2010, 17, 870-877.	3.8	64

#	Article	IF	CITATIONS
91	Synthesis and characterization of FeSe2 nanoparticles and FeSe2/FeO(OH) nanocomposites by hydrothermal method. Journal of Alloys and Compounds, 2015, 625, 26-33.	2.8	64
92	Synthesis and characterization of hexagonal nano-sized nickel selenide by simple hydrothermal method assisted by CTAB. Applied Surface Science, 2011, 257, 7982-7987.	3.1	61
93	Synthesis, characterization and investigation of the electrochemical hydrogen storage properties of CuO–CeO2 nanocomposites synthesized by green method. International Journal of Hydrogen Energy, 2017, 42, 14608-14620.	3.8	61
94	Utilizing of neodymium vanadate nanoparticles as an efficient catalyst to boost the photocatalytic water purification. Journal of Environmental Management, 2019, 230, 266-281.	3.8	59
95	Shape control of nickel selenides synthesized by a simple hydrothermal reduction process. Polyhedron, 2012, 31, 210-216.	1.0	58
96	Synthesis and Characterization of Al(OH)3, Al2O3 Nanoparticles and Polymeric Nanocomposites. Journal of Cluster Science, 2016, 27, 25-38.	1.7	57
97	Particle size and shape modification of hydroxyapatite nanostructures synthesized via a complexing agent-assisted route. Materials Science and Engineering C, 2014, 40, 288-298.	3.8	55
98	Lead hexaferrite nanostructures: green amino acid sol–gel auto-combustion synthesis, characterization and considering magnetic property. Journal of Materials Science: Materials in Electronics, 2017, 28, 17627-17634.	1.1	55
99	Photodegradation and removal of organic dyes using cui nanostructures, green synthesis and characterization. Separation and Purification Technology, 2017, 173, 27-36.	3.9	53
100	Effect of nickel salt precursors on morphology, size, optical property and type of products (NiSe or) Tj ETQq0 0 C	) rgBT /Ov 1.7	erlock 10 Tf 50
101	Rapid and green combustion synthesis of nanocomposites based on Zn–Co–O nanostructures as photocatalysts for enhanced degradation of acid brown 14 contaminant under sunlight. Separation and Purification Technology, 2022, 280, 119841.	3.9	51
102	Porous hollow Ag/Ag2S/Ag3PO4 nanocomposites as highly efficient heterojunction photocatalysts for the removal of antibiotics under simulated sunlight irradiation. Chemosphere, 2021, 274, 129765.	4.2	49
103	Sonochemical synthesis of SrMnO3 nanoparticles as an efficient and new catalyst for O2 evolution from water splitting reaction. Ultrasonics Sonochemistry, 2018, 40, 651-663.	3.8	48
104	Effect of copper phthalocyanine (CuPc) on electrochemical hydrogen storage capacity of BaAl2O4/BaCO3 nanoparticles. International Journal of Hydrogen Energy, 2017, 42, 15308-15318.	3.8	45
105	Dy3Fe5O12 and DyFeO3 nanostructures: Green and facial auto-combustion synthesis, characterization and comparative study on electrochemical hydrogen storage. International Journal of Hydrogen Energy, 2018, 43, 9713-9721.	3.8	45
106	New Nanocomposites Based on Li–Fe–Mn Double Spinel and Carbon Self-Doped Graphitic Carbon Nitrides with Synergistic Effect for Electrochemical Hydrogen Storage Application. Industrial & Engineering Chemistry Research, 2019, 58, 23057-23067.	1.8	45
107	BaMnO3 nanostructures: Simple ultrasonic fabrication and novel catalytic agent toward oxygen evolution of water splitting reaction. Ultrasonics Sonochemistry, 2020, 61, 104829.	3.8	45
108	Green synthesis and characterization of cerium oxide nanostructures in the presence carbohydrate sugars as a capping agent and investigation of their cytotoxicity on the mesenchymal stem cell. Journal of Cleaner Production, 2017, 156, 741-749.	4.6	44

#	Article	IF	CITATIONS
109	Sol-Gel auto-combustion synthesis and physicochemical properties of BaAl2O4 nanoparticles; electrochemical hydrogen storage performance and density functional theory. Renewable Energy, 2017, 114, 1419-1426.	4.3	44
110	Strategic design and electrochemical behaviors of Li-ion battery cathode nanocomposite materials based on AlV3O9 with carbon nanostructures. Composites Part B: Engineering, 2020, 183, 107734.	5.9	44
111	Zinc oxide nanoparticles: solvent-free synthesis, characterization and application as heterogeneous nanocatalyst for photodegradation of dye from aqueous phase. Journal of Materials Science: Materials in Electronics, 2017, 28, 8423-8428.	1.1	43
112	Facile fabrication of Tl <sub>4</sub> Hgl <sub>6</sub> nanostructures as novel antibacterial and antibiofilm agents and photocatalysts in the degradation of organic pollutants. Inorganic Chemistry Frontiers, 2021, 8, 2442-2460.	3.0	43
113	Green facile thermal decomposition synthesis, characterization and electrochemical hydrogen storage characteristics of ZnAl2O4 nanostructure. International Journal of Hydrogen Energy, 2017, 42, 17167-17177.	3.8	42
114	Pechini sol-gel synthesis of Cu2O/Li3BO3 and CuO/Li3BO3 nanocomposites for visible light-driven photocatalytic degradation of dye pollutant. Journal of Alloys and Compounds, 2020, 815, 152451.	2.8	42
115	Synthesis and Characterization of Bis(Macrocyclic) Nickel(II) Complexes Containing Aromatic Nitrogen–Nitrogen Linkers Produced by Template Condensation. Transition Metal Chemistry, 2006, 31, 157-162.	0.7	41
116	Simple synthesis and characterization of Ag 2 CdI 4 /AgI nanocomposite as an effective photocatalyst by co-precipitation method. Journal of Molecular Liquids, 2016, 223, 21-28.	2.3	41
117	Thermosensitive alginate–gelatin–nitrogen-doped carbon dots scaffolds as potential injectable hydrogels for cartilage tissue engineering applications. RSC Advances, 2021, 11, 18423-18431.	1.7	41
118	A new simple route for the preparation of nanosized copper selenides under different conditions. Ceramics International, 2014, 40, 8173-8182.	2.3	40
119	Green synthesis of flower-like Cul microstructures composed of trigonal nanostructures using pomegranate juice. Materials Letters, 2013, 100, 133-136.	1.3	39
120	Photocatalytic degradation of methylene blue on TiO2@SiO2 core/shell nanoparticles: synthesis and characterization. Journal of Materials Science: Materials in Electronics, 2015, 26, 6170-6177.	1.1	39
121	Synthesis, characterization, optical and magnetic properties of a nickel sulfide series by three different methods. Superlattices and Microstructures, 2013, 59, 1-12.	1.4	38
122	Photo-catalyst tin dioxide: synthesis and characterization different morphologies of SnO2 nanostructures and nanocomposites. Journal of Materials Science: Materials in Electronics, 2015, 26, 6970-6978.	1.1	38
123	Thermal decomposition synthesis, characterization and electrochemical hydrogen storage characteristics of Co3O4–CeO2 porous nanocomposite. International Journal of Hydrogen Energy, 2017, 42, 20071-20081.	3.8	38
124	Synthesis, characterization and antibacterial activities of Ni/ZnO nanocomposites using bis(salicylaldehyde) complex precursor. Journal of Alloys and Compounds, 2019, 788, 383-390.	2.8	37
125	Morphological control of MnSe2/Se nanocomposites by amount of hydrazine through a hydrothermal process. Materials Research Bulletin, 2013, 48, 3204-3210.	2.7	36
126	Synthesis and characterization of CdSe nanostructures by using a new selenium source: Effect of hydrothermal preparation conditions. Materials Research Bulletin, 2014, 53, 7-14.	2.7	36

#	Article	IF	CITATIONS
127	Two facile methods to produce the cobalt manganite nanostructures and evaluation of their photocatalytic performance. Journal of Materials Science: Materials in Electronics, 2017, 28, 6292-6300.	1.1	36
128	Effect of preparation conditions on synthesis of Ag2Se nanoparticles by simple sonochemical method assisted by thiourea. Journal of Industrial and Engineering Chemistry, 2014, 20, 3775-3779.	2.9	35
129	Hydrothermal synthesis, characterization, and magnetic properties of cubic MnSe 2 /Se nanocomposites material. Journal of Alloys and Compounds, 2014, 617, 93-101.	2.8	35
130	Novel precursors for synthesis of dendrite-like PbTe nanostructures and investigation of photoluminescence behavior. Advanced Powder Technology, 2014, 25, 1585-1592.	2.0	35
131	Ultrasonic assisted synthesis of a nano-sized Co2SnO4/graphene: A potential material for electrochemical hydrogen storage application. International Journal of Hydrogen Energy, 2018, 43, 4381-4392.	3.8	35
132	Using pomegranate peel powders as a new capping agent for synthesis of CuO/ZnO/Al2O3 nanostructures; enhancement of visible light photocatalytic activity. International Journal of Hydrogen Energy, 2018, 43, 14406-14416.	3.8	34
133	Structural characterization and electrochemical hydrogen sorption performances of the polycrystalline Ba2Co9O14 nanostructures. Journal of Alloys and Compounds, 2019, 777, 252-258.	2.8	34
134	Fabrication of S-scheme ZnO/Zn3(PO4)2 heterojunction photocatalyst toward photodegradation of tetracycline antibiotic and photocatalytic mechanism insight. International Journal of Hydrogen Energy, 2022, 47, 928-939.	3.8	34
135	Sodium dodecyl benzene sulfonate-assisted synthesis through a hydrothermal reaction. Materials Research Bulletin, 2012, 47, 1905-1911.	2.7	33
136	The effect of Cul–Pbl2 nanocomposite fabricated by the sonochemical route on electrochemical hydrogen storage characteristics. International Journal of Hydrogen Energy, 2021, 46, 19074-19084.	3.8	33
137	Efficient degradation of azo dye pollutants on ZnBi38O58 nanostructures under visible-light irradiation. Separation and Purification Technology, 2018, 195, 30-36.	3.9	32
138	Synthesis and characterisation of cadmium selenide nanostructures by simple sonochemical method. Micro and Nano Letters, 2012, 7, 831.	0.6	31
139	Novel and solvent-free cochineal-assisted synthesis of Ag–Al2O3 nanocomposites via solid-state thermal decomposition route: characterization and photocatalytic activity assessment. Journal of Materials Science: Materials in Electronics, 2016, 27, 9789-9797.	1.1	31
140	Controlled green synthesis and characterization of CeO2 nanostructures as materials for the determination of ascorbic acid. Journal of Molecular Liquids, 2017, 241, 772-781.	2.3	31
141	Sol-gel synthesis of novel Li-based boron oxides nanocomposite for photodegradation of azo-dye pollutant under UV light irradiation. Composites Part B: Engineering, 2019, 172, 33-40.	5.9	31
142	Green sol–gel auto combustion synthesis and characterization of double perovskite Tb <sub>2</sub> ZnMnO <sub>6</sub> nanoparticles and a brief study of photocatalytic activity. RSC Advances, 2021, 11, 8228-8238.	1.7	31
143	Pechini synthesis and characteristics of Gd2CoMnO6 nanostructures and its structural, optical and photocatalytic properties. Spectrochimica Acta - Part A: Molecular and Biomolecular Spectroscopy, 2018, 204, 232-240.	2.0	31
144	Controllable synthesis of new Tl2S2O3 nanostructures via hydrothermal process; characterization and investigation photocatalytic activity for degradation of some anionic dyes. Journal of Molecular Liquids, 2016, 219, 851-857.	2.3	30

#	Article	IF	CITATIONS
145	Urchin-like Dy2CoMnO6 double perovskite nanostructures: new simple fabrication and investigation of their photocatalytic properties. Journal of Materials Science: Materials in Electronics, 2017, 28, 12440-12447.	1.1	30
146	The impact of zirconium oxide nanoparticles content on alginate dialdehyde-gelatin scaffolds in cartilage tissue engineering. Journal of Molecular Liquids, 2021, 335, 116531.	2.3	30
147	Template Syntheses Involving the Carbon Acid Nitroethane. Synthesis and Characterization of Copper(II) Complexes of a 16-membered Tetraaza Macrocycle. Transition Metal Chemistry, 2005, 30, 720-725.	0.7	29
148	Bis(macrocyclic)dinickel(II) complexes containing phenylene bridges between 13-membered triaza dioxa macrocyclic ligands: in-situ one pot template synthesis, characterization and catalytic oxidation of cyclohexene. Transition Metal Chemistry, 2007, 32, 9-15.	0.7	29
149	Ag2Cdl4: Synthesis, characterization and investigation the strain lattice and grain size. Journal of Alloys and Compounds, 2016, 667, 115-122.	2.8	29
150	Investigation of Mn2O3 as impurity on the electrochemical hydrogen storage performance of MnO2CeO2 nanocomposites. International Journal of Hydrogen Energy, 2017, 42, 28473-28484.	3.8	29
151	<i>In vitro</i> study of alginate–gelatin scaffolds incorporated with silica NPs as injectable, biodegradable hydrogels. RSC Advances, 2021, 11, 16688-16697.	1.7	29
152	Comparative study on electrochemical hydrogen storage of nanocomposites based on S or N doped graphene quantum dots and nanostructured titanium niobate. Journal of Alloys and Compounds, 2022, 899, 163379.	2.8	29
153	Improved pechini sol-gel fabrication of Li2B4O7/NiO/Ni3(BO3)2 nanocomposites to advanced photocatalytic performance. Arabian Journal of Chemistry, 2022, 15, 103768.	2.3	29
154	Cubic HgSe nanoparticles: sonochemical synthesis and characterisation. Micro and Nano Letters, 2012, 7, 1300-1304.	0.6	28
155	Single-Source Molecular Precursor for Synthesis of Copper Sulfide Nanostructures. Journal of Cluster Science, 2012, 23, 1143-1151.	1.7	28
156	Influence of morphology on the in vitro bioactivity of hydroxyapatite nanostructures prepared by precipitation method. New Journal of Chemistry, 2014, 38, 4501.	1.4	28
157	Sonochemical-assisted route for synthesis of spherical shaped holmium vanadate nanocatalyst for polluted waste water treatment. Ultrasonics Sonochemistry, 2019, 58, 104686.	3.8	28
158	Facile synthesis of Au/ZnO/RGO nanohybrids using 1,8-diamino-3,6-dioxaoctan as novel functional agent for photo-degradation water treatment. Journal of Materials Research and Technology, 2021, 15, 6098-6112.	2.6	28
159	Cobalt selenide nanostructures: Hydrothermal synthesis, considering the magnetic property and effect of the different synthesis conditions. Journal of Molecular Liquids, 2016, 219, 1089-1094.	2.3	27
160	Ultrasound-accelerated synthesis of uniform DyVO4 nanoparticles as high activity visible-light-driven photocatalyst. Ultrasonics Sonochemistry, 2019, 59, 104719.	3.8	27
161	CdSnO3-graphene nanocomposites: Ultrasonic synthesis using glucose as capping agent and characterization for electrochemical hydrogen storage. Ultrasonics Sonochemistry, 2020, 61, 104840.	3.8	27
162	Hydrothermal Synthesis of Spinel-Perovskite Li–Mn–Fe–Si Nanocomposites for Electrochemical Hydrogen Storage. Inorganic Chemistry, 2022, 61, 6750-6763.	1.9	27

#	Article	IF	CITATIONS
163	Hydrothermal preparation of silver telluride nanostructures and photo-catalytic investigation in degradation of toxic dyes. Scientific Reports, 2016, 6, 20060.	1.6	26
164	Morphology-controlled synthesis, characterization and photocatalytic property of hierarchical flower-like Dy2Mo3O9 nanostructures. Journal of Materials Science: Materials in Electronics, 2017, 28, 10313-10320.	1.1	26
165	Highly Selective Ratiometric Fluorescent Sensor for La(III) Ion Based on a New Schiff's Base. Analytical Letters, 2009, 42, 1029-1040.	1.0	25
166	MgCr2O4 and MgCr2O4/Ag nanostructures: Facile size-controlled synthesis and their photocatalytic performance for destruction of organic contaminants― Composites Part B: Engineering, 2019, 175, 107077.	5.9	25
167	The first synthesis of CdFe12O19 nanostructures and nanocomposites and considering of magnetic, optical, electrochemical and photocatalytic properties. Journal of Hazardous Materials, 2019, 367, 607-619.	6.5	25
168	Magnetite as Inorganic Hole Transport Material for Lead Halide Perovskite-Based Solar Cells with Enhanced Stability. Industrial & Engineering Chemistry Research, 2020, 59, 743-750.	1.8	25
169	Copper(II) complexes with 18-membered decaaza macrocycles: synthesis, characterization and catalytic activity. Transition Metal Chemistry, 2005, 30, 445-450.	0.7	24
170	Sonochemical synthesis of HgSe nanoparticles: Effect of metal salt, reaction time and reductant agent. Journal of Industrial and Engineering Chemistry, 2014, 20, 3518-3523.	2.9	24
171	Synthesis and characterization of ceria nanostructures with different morphologies via a simple thermal decompose method with different cerium complexes and investigation the photocatalytic activity. Journal of Materials Science: Materials in Electronics, 2016, 27, 8793-8801.	1.1	24
172	Optimized synthesis of ZnSe nanocrystals by hydrothermal method. Journal of Materials Science: Materials in Electronics, 2016, 27, 293-303.	1.1	24
173	Dy2O3/CuO nanocomposites: microwave assisted synthesis and investigated photocatalytic properties. Journal of Materials Science: Materials in Electronics, 2018, 29, 1238-1245.	1.1	24
174	Electrochemical hydrogen storage properties of Ce0.75Zr0.25O2 nanopowders synthesized by sol-gel method. Journal of Alloys and Compounds, 2019, 790, 884-890.	2.8	24
175	Superhydrophobic–superoleophilic copper–graphite/styrene–butadiene–styrene based cotton filter for efficient separation of oil derivatives from aqueous mixtures. Cellulose, 2020, 27, 4691-4705.	2.4	24
176	Synergic and coupling effect between SnO <sub>2</sub> nanoparticles and hierarchical AlV <sub>3</sub> O <sub>9</sub> microspheres toward emerging electrode materials for lithium-ion battery devices. Inorganic Chemistry Frontiers, 2021, 8, 2735-2748.	3.0	24
177	Visible light-induced degradation of amoxicillin antibiotic by novel CuI/FePO4 p-n heterojunction photocatalyst and photodegradation mechanism. Journal of Alloys and Compounds, 2022, 892, 162176.	2.8	24
178	Effect of Operational Synthesis Parameters on the Morphology and the Electrochemical Properties of 3D Hierarchical AlV <sub>3</sub> O <sub>9</sub> Architectures for Li-Ion Batteries. Journal of the Electrochemical Society, 2020, 167, 020544.	1.3	24
179	A facile hydrothermal method for synthesis different morphologies of PbTe nanostructures. Journal of Industrial and Engineering Chemistry, 2014, 20, 3335-3341.	2.9	23
180	CdSe nanoparticles: facile hydrothermal synthesis, characterization and optical properties. Journal of Materials Science: Materials in Electronics, 2015, 26, 6831-6836.	1.1	23

#	Article	IF	CITATIONS
181	Co2SiO4 nanostructures/nanocomposites: synthesis and investigations of optical, magnetic, photocatalytic, thermal stability and flame retardant properties. Journal of Materials Science: Materials in Electronics, 2018, 29, 7077-7089.	1.1	23
182	Structural and spectroscopic characterization of HgS nanoparticles prepared via simple microwave approach in presence of novel sulfuring agent. Transactions of Nonferrous Metals Society of China, 2016, 26, 759-766.	1.7	22
183	Silver selenide nanoparticles: synthesis, characterisation and effect of preparation conditions under ultrasound radiation. Micro and Nano Letters, 2013, 8, 508-511.	0.6	21
184	Preparation and Characterization of PbS Nanoparticles via Cyclic Microwave Radiation Using Precursor of Lead (II) Oxalate. Journal of Cluster Science, 2014, 25, 937-947.	1.7	21
185	Pechini synthesis of Co2SiO4 magnetic nanoparticles and its application in photo-degradation of azo dyes. Journal of Molecular Liquids, 2016, 220, 223-231.	2.3	21
186	Green sol-gel auto-combustion synthesis, characterization and investigation of the electrochemical hydrogen storage properties of barium cobalt oxide nanocomposites with maltose. International Journal of Hydrogen Energy, 2020, 45, 17662-17670.	3.8	21
187	Simple preparation of chitosan-coated thallium lead iodide nanostructures as a new visible-light photocatalyst in decolorization of organic contamination. Journal of Molecular Liquids, 2021, 341, 117299.	2.3	21
188	Green synthesis of SrFe12O19@Ag and SrFe12O19@Au as magnetic plasmonic nanocomposites with high photocatalytic performance for degradation of organic pollutants. Chemosphere, 2022, 291, 132741.	4.2	21
189	Drug delivery based on chitosan, β-cyclodextrin and sodium carboxymethyl cellulose as well as nanocarriers for advanced leukemia treatment. Biomedicine and Pharmacotherapy, 2022, 153, 113369.	2.5	21
190	Determination of zinc in water samples by flame atomic absorption spectrometry after homogeneous liquid-liquid extraction. Journal of Analytical Chemistry, 2011, 66, 612-617.	0.4	20
191	Amino acid modified combustion synthesis, characterization and investigation of magnetic, optical and photocatalytic properties of Gd2CoMnO6 nanostructures. Journal of Alloys and Compounds, 2018, 753, 615-621.	2.8	20
192	Photocatalytic degradation of diverse organic dyes by sol–gel synthesized Cd2V2O7 nanostructures. Journal of Materials Science: Materials in Electronics, 2018, 29, 18120-18127.	1.1	20
193	Synthesis of different morphologies of Cu2Cdl4/Cul nanocomposite via simple hydrothermal method. Journal of Materials Science: Materials in Electronics, 2016, 27, 11092-11101.	1.1	19
194	Thermal treatment synthesis of SnO2 nanoparticles and investigation of its light harvesting application. Applied Physics A: Materials Science and Processing, 2016, 122, 1.	1.1	19
195	Green sonochemistry assisted synthesis of hollow magnetic and photoluminescent MgFe <sub>2</sub> O <sub>4</sub> –carbon dot nanocomposite as a sensor for toxic Ni( <scp>ii</scp> ), Cd( <scp>ii</scp> ) and Hg( <scp>ii</scp> ) ions and bacteria. RSC Advances, 2021, 11, 22805-22811.	1.7	19
196	Fabrication of an iron(III)-selective PVC membrane sensor based on a bis-bidentate Schiff base ionophore. Transition Metal Chemistry, 2008, 33, 995-1001.	0.7	18
197	Sonochemical preparation of pure t-LaVO4 nanoparticles with the aid of tris(acetylacetonato)lanthanum hydrate as a novel precursor. Ultrasonics Sonochemistry, 2014, 21, 653-662.	3.8	18
198	A reliable hydrophobic/superoleophilic fabric filter for oil–water separation: hierarchical bismuth/purified terephthalic acid nanocomposite. Cellulose, 2020, 27, 9559-9575.	2.4	18

#	Article	IF	CITATIONS
199	Facile One-Pot In Situ Synthesis and Characterization of a Cu <sub>2</sub> O/Cu <sub>2</sub> (PO <sub>4</sub> )(OH) Binary Heterojunction Nanocomposite for the Efficient Photocatalytic Degradation of Ciprofloxacin from Aqueous Solution under Direct Sunlight Irradiation. Industrial & amp; Engineering Chemistry Research, 2021, 60, 9578-9591.	1.8	18
200	La2Sn2O7/g-C3N4 nanocomposites: Rapid and green sonochemical fabrication and photo-degradation performance for removal of dye contaminations. Ultrasonics Sonochemistry, 2021, 77, 105678.	3.8	18
201	Synthesis and investigation of physicochemical properties of alginate dialdehyde/gelatin/ZnO nanocomposites as injectable hydrogels. Polymer Testing, 2022, 110, 107562.	2.3	18
202	Synthesis and Characterization of Silver Selenide Nanoparticles via a Facile Sonochemical Route Starting from a Novel Inorganic Precursor. Journal of Inorganic and Organometallic Polymers and Materials, 2013, 23, 357-364.	1.9	17
203	AgSCN micro/nanostructures: Facile sonochemical synthesis, characterization, and photoluminescence properties. Journal of Industrial and Engineering Chemistry, 2014, 20, 3780-3788.	2.9	17
204	Long-Term Durability of Bromide-Incorporated Perovskite Solar Cells via a Modified Vapor-Assisted Solution Process. ACS Applied Energy Materials, 2018, 1, 6018-6026.	2.5	17
205	Fe <sub>2</sub> O <sub>3</sub> –CeO <sub>2</sub> Ceramic Nanocomposite Oxide: Characterization and Investigation of the Effect of Morphology on Its Electrochemical Hydrogen Storage Capacity. ACS Applied Energy Materials, 2018, 1, 4840-4848.	2.5	17
206	Sonochemical-assisted synthesis of pure Dy2ZnMnO6 nanoparticles as a novel double perovskite and study of photocatalytic performance for wastewater treatment. Ultrasonics Sonochemistry, 2019, 57, 172-184.	3.8	17
207	Investigation of photocatalytic, electrochemical, optical and magnetic behaviors of rare-earth double perovskites using combustion synthesized Gd2NiMnO6 nanostructures in the presence of different saccharides. International Journal of Hydrogen Energy, 2019, 44, 860-869.	3.8	17
208	Controlled synthesis of Tl2O3 nanostructures via microwave route by a novel pH adjuster and investigation of its photocatalytic activity. Journal of Materials Science: Materials in Electronics, 2015, 26, 5326-5334.	1.1	16
209	Synthesis and characterization of Ag2CdI4 nanoparticles and photo-degradation of organic dyes. Journal of Materials Science: Materials in Electronics, 2017, 28, 6272-6277.	1.1	16
210	Pechini synthesis using propylene glycol and various acid as stabilizing agents and characterization of Gd2NiMnO6 ceramic nanostructures with good photocatalytic properties for removal of organic dyes in water. Journal of Materials Research and Technology, 2020, 9, 1720-1733.	2.6	16
211	Barium cobaltite nanoparticles: Sol-gel synthesis and characterization and their electrochemical hydrogen storage properties. International Journal of Hydrogen Energy, 2021, 46, 886-895.	3.8	16
212	Photo-catalyst thallium sulfide: synthesis and optical characterization different morphologies of Tl2S nanostructures. Journal of Materials Science: Materials in Electronics, 2015, 26, 8798-8806.	1.1	15
213	Toxic effects of Fe2WO6 nanoparticles towards microalga Dunaliella salina: Sonochemical synthesis nanoparticles and investigate its impact on the growth. Chemosphere, 2020, 258, 127348.	4.2	14
214	ZnCo2O4/ZnO nanocomposite: Facile one-step green solid-state thermal decomposition synthesis using Dactylopius Coccus as capping agent, characterization and its 4T1 cells cytotoxicity investigation and anticancer activity. Arabian Journal of Chemistry, 2021, 14, 103316.	2.3	14
215	Photocatalytic degradation of antibiotic using Ni-doped thallium(I) orthotungstate nanorods: Hydrothermal synthesis and characterization. Journal of Alloys and Compounds, 2021, 874, 159856.	2.8	14
216	Separation and Preconcentration of Trace Gallium and Indium by Amberlite XAD-7 Resin Impregnated with a New Hexadentates Naphthol-Derivative Schiff Base. Separation Science and Technology, 2009, 44, 1851-1868.	1.3	13

#	Article	IF	CITATIONS
217	Extraction and preconcentration of ultra trace amounts of beryllium from aqueous samples by nanometer mesoporous silica functionalized by 2,4-dihydroxybenzaldehyde prior to ICP OES determination. Mikrochimica Acta, 2010, 169, 241-248.	2.5	13
218	Single-Source Molecular Precursor for Synthesis of CdS Nanoparticles and Nanoflowers. High Temperature Materials and Processes, 2012, 31, .	0.6	13
219	Simple synthesis and characterization of nickel phosphide nanostructures assisted by different inorganic precursors. Journal of Materials Science: Materials in Electronics, 2016, 27, 3619-3627.	1.1	13
220	Study on the optical, magnetic, and photocatalytic activities of the synthesized Mn2O3-SiO2 nanocomposites by microwave method. Journal of Molecular Liquids, 2017, 242, 779-788.	2.3	13
221	Sonochemical synthesis, characterization and investigation of the electrochemical hydrogen storage properties of TIPbI3/Tl4PbI6 nanocomposite. International Journal of Hydrogen Energy, 2021, 46, 6648-6658.	3.8	13
222	Fabrication of TlSnI3/C3N4 nanocomposites for enhanced photodegradation of toxic contaminants below visible light and investigation of kinetic and mechanism of photocatalytic reaction. Journal of Molecular Liquids, 2022, 349, 118443.	2.3	13
223	Synthesis and characterization of carbon sphere-supported sand-rose like N-GQDs/NiCo2S4 structures with synergetic effect for development of hydrogen storage capacity. Fuel, 2022, 312, 122956.	3.4	13
224	Green fabrication of graphene quantum dots from cotton with CaSiO3 nanostructure and enhanced photocatalytic performance for water treatment. International Journal of Hydrogen Energy, 2022, 47, 7228-7241.	3.8	13
225	Decoration of green synthesized S, N-GQDs and CoFe2O4 on halloysite nanoclay as natural substrate for electrochemical hydrogen storage application. Scientific Reports, 2022, 12, 8103.	1.6	13
226	Co2SiO4 nanostructures: New simple synthesis, characterization and investigation of optical property. Materials Research Bulletin, 2017, 88, 248-257.	2.7	12
227	Sol–gel auto combustion synthesis of BaFe18O27 nanostructures for adsorptive desulfurization of liquid fuels. International Journal of Hydrogen Energy, 2017, 42, 12320-12326.	3.8	12
228	Simple sol–gel green auto combustion synthesis by using carbohydrate sugars as a novel reducing agent, characterization, photocatalytic behavior and slow-burning property of Ni2SiO4 nanocomposites. Journal of Materials Science: Materials in Electronics, 2017, 28, 16981-16991.	1.1	12
229	Mechanosynthesis and characterization AFe2O4 (A: Ni, Cu, Zn)-activated carbon nanocomposite as an effective adsorbent for removal dodecanethiol. Microporous and Mesoporous Materials, 2018, 262, 13-22.	2.2	12
230	Green synthesis and characterization of MnCo2O4/Co2Mn3O8 ceramic nanocomposites and investigation of their cytotoxicity on the 4T1 cells. Composites Part B: Engineering, 2019, 163, 424-430.	5.9	12
231	Li2MnO3/LiMnBO3/MnFe2O4 ternary nanocomposites: Pechini synthesis, characterization and photocatalytic performance. International Journal of Hydrogen Energy, 2020, 45, 21241-21251.	3.8	12
232	Role of morphology in electrochemical hydrogen storage using binary DyFeO3-ZnO nanocomposites as electrode materials. International Journal of Hydrogen Energy, 2021, 46, 21026-21039.	3.8	12
233	Morphology engineering of LiFeO2 nanostructures through synthesis controlling for electrochemical hydrogen storage inquiries. Fuel, 2022, 313, 123025.	3.4	12
234	Hydrothermal synthesis of CoSe nanostructures without using surfactant. Journal of Molecular Liquids, 2016, 220, 334-338.	2.3	11

#	Article	IF	CITATIONS
235	Zn2MnO4/ZnO nanocomposites: One step sonochemical fabrication and demonstration as a novel catalyst in water splitting reaction. Ceramics International, 2020, 46, 25789-25801.	2.3	11
236	Unveiling the synthesis of CuCe2(MoO4)4 nanostructures and its physico-chemical properties on electrochemical hydrogen storage. Journal of Alloys and Compounds, 2020, 826, 154023.	2.8	11
237	Controllable synthesis and characterization of Mg <sub>2</sub> SiO <sub>4</sub> nanostructures <i>via</i> a simple hydrothermal route using carboxylic acid as capping agent and their photocatalytic performance for photodegradation of azo dyes. RSC Advances, 2021, 11, 21588-21599.	1.7	11
238	Synthesis, characterization, and catalytic oxidation of ethylbenzene over host (zeolite-Y)/guest (copper(II) complexes of tetraaza macrocyclic ligands) nanocomposite materials. Journal of Coordination Chemistry, 2010, 63, 3240-3255.	0.8	10
239	Photo-degradation of organic dyes: simple chemical synthesis of various morphologies of tin dioxide semiconductor and its nanocomposite. Journal of Materials Science: Materials in Electronics, 2015, 26, 6075-6085.	1.1	10
240	Photoluminescence, photocatalytic and solar cell behaviors of as-prepared Germania nanoparticles from a sol–gel route. Journal of Materials Science: Materials in Electronics, 2015, 26, 5822-5832.	1.1	10
241	Synthesis and characterization of mercury telluride nanoparticles using a new precursor. Journal of Industrial and Engineering Chemistry, 2014, 20, 3415-3420.	2.9	9
242	Synthesis of Co2P/Co nanocomposites using single source precursor by thermal decomposition method. Journal of Materials Science: Materials in Electronics, 2016, 27, 3271-3280.	1.1	9
243	Sol-gel synthesis and characterization of Co3O4/CeO2 nanocomposites and its application for photocatalytic discoloration of organic dye from aqueous solutions. Environmental Science and Pollution Research, 2021, 28, 7001-7015.	2.7	9
244	DyMnO3/Fe2O3 nanocomposites: simple sol-gel auto-combustion technique and photocatalytic performance for water treatment. Environmental Science and Pollution Research, 2021, 28, 11066-11076.	2.7	9
245	Interfacial Passivation of Perovskite Solar Cells by Reactive Ion Scavengers. ACS Applied Energy Materials, 2021, 4, 1078-1084.	2.5	9
246	Effect of g-C3N4 amount on green synthesized GdFeO3/g-C3N4 nanocomposites as promising compounds for solid-state hydrogen storage. International Journal of Hydrogen Energy, 2023, 48, 6586-6596.	3.8	9
247	New avenue for preparation of potential hydrogen storage materials based on K10 montmorillonite and Ca2Mn3O8/CaMn3O6 nanocomposites. Fuel, 2022, 320, 123933.	3.4	9
248	Highly Selective and Sensitive Tin(II) Membrane Electrode Based on a New Synthesized Schiff's Base. Electroanalysis, 2009, 21, 859-866.	1.5	8
249	Fabrication and characterization of molybdenum(VI)complex-TiO2 nanoparticles modified electrode for the electrocatalytic determination of L-cysteine. Journal of the Serbian Chemical Society, 2011, 76, 575-589.	0.4	8
250	Synthesis and Characterization of CdCO3 Nanostructures via Simple Hydrothermal Method. Journal of Cluster Science, 2013, 24, 1-9.	1.7	8
251	Synthesis of bismuth sulfide nanostructures by using bismuth(III) monosalicylate precursor and fabrication of bismuth sulfide based p–n junction solar cells. Asia-Pacific Journal of Chemical Engineering, 2014, 9, 16-23.	0.8	8
252	Synthesis, characterization and photovoltaic studies of CulnS2 nanostructures. Journal of Materials Science: Materials in Electronics, 2015, 26, 2810-2819.	1.1	8

#	Article	IF	CITATIONS
253	A Simple Sonochemical Route for Synthesis Silver Selenide Nanoparticles From SeCl <sub>4</sub> and Silver Salicylate. Synthesis and Reactivity in Inorganic, Metal Organic, and Nano Metal Chemistry, 2015, 45, 58-67.	0.6	8
254	Characterization of hydrogen storage behavior of the as-synthesized p-type NiO/n-type CeO2 nanocomposites by carbohydrates as a capping agent: The influence of morphology. International Journal of Hydrogen Energy, 2018, 43, 14557-14568.	3.8	8
255	A study on electrochemical hydrogen storage properties of truncated octahedron cobalt cerium molybdate nanocrystals synthesized by solution combustion method. Journal of Alloys and Compounds, 2021, 858, 158374.	2.8	8
256	Preparation and study of characteristics of LiCoO <sub>2</sub> /Fe <sub>3</sub> O <sub>4</sub> /Li <sub>2</sub> B <sub>2</sub> O <sub>4</sub> nanocomposites as ideal active materials for electrochemical hydrogen storage. RSC Advances, 2021, 11, 23430-23436.	1.7	8
257	Synthesis of calcium manganese oxide with different constructions as potential materials for electrochemical hydrogen storage. Fuel, 2022, 321, 124074.	3.4	8
258	Sol-gel auto-combustion synthesis of a novel chitosan/Ho2Ti2O7 nanocomposite and its characterization for photocatalytic degradation of organic pollutant in wastewater under visible illumination. International Journal of Hydrogen Energy, 2022, 47, 21146-21159.	3.8	8
259	Sonochemical synthesis and characterization of CuInS2 nanostructures using new sulfur precursor and their application as photocatalyst for degradation of organic pollutants under simulated sunlight. Arabian Journal of Chemistry, 2022, 15, 104007.	2.3	8
260	Adsorptive desulfurization of model fuels using ferrite nickel-silica in continues system: Modelling of breakthrough curves, thermodynamic study and experimental design. Fuel, 2022, 327, 124999.	3.4	8
	Synthesis, characterization and catalytic oxidation of cyclohexene with molecular oxygen over host		

0.6

4

#	Article	IF	CITATIONS
271	Synthesis and characterization of ZnO–Ce nanophotocatalyst and their application for the removal of dye (Reactive red 198) by degradation process: Kinetics, thermodynamics and experimental design. International Journal of Hydrogen Energy, 2022, 47, 23980-23993.	3.8	7
272	Synthesis and Characterization of CdS Nanoparticles via Cyclic Microwave from Cadmium Oxalate. Journal of Cluster Science, 2013, 24, 299-313.	1.7	6
273	Synthesis and characterization of PbTe micro/nanostructures through hydrothermal method by using a novel capping agent. Bulletin of Materials Science, 2014, 37, 753-759.	0.8	6
274	Synthesis and Characterization of Barium Carbonate Nanostructures Via Simple Hydrothermal Method. Synthesis and Reactivity in Inorganic, Metal Organic, and Nano Metal Chemistry, 2016, 46, 317-322.	0.6	6
275	Hydrothermal synthesis and characterization of lead oxide nanocrystal in presence of tetradentate Schiff-base and degradation investigation of organic pollutant in waste water. Journal of Materials Science: Materials in Electronics, 2017, 28, 9919-9926.	1.1	6
276	PbHgI4/HgI2 nanocomposite: simple synthesis, characterization and electrochemical and optical properties. Journal of Materials Science: Materials in Electronics, 2017, 28, 2615-2623.	1.1	6
277	Lead carbonate hydroxide nanostructures: a new hydrothermal synthesis in the presence of ethylenediamine and hydrazine and investigation photocatalytic behavior. Journal of Materials Science: Materials in Electronics, 2019, 30, 20947-20957.	1.1	6
278	Tb2CoMnO6 double perovskites nanoparticles as photocatalyst for the degradation of organic dyes: Synthesis and characterization. Arabian Journal of Chemistry, 2021, 14, 103349.	2.3	6
279	Nanocomposite scaffolds based on gelatin and alginate reinforced by Zn2SiO4 with enhanced mechanical and chemical properties for tissue engineering. Arabian Journal of Chemistry, 2022, 15, 103730.	2.3	6
280	Host (nanopores of zeolite-Y)/guest (Co(II)-azamacrocyclic complexes) nanocomposite materials: synthesis, characterization and catalytic epoxidation of styrene with molecular oxygen. Journal of Coordination Chemistry, 2008, 61, 2837-2851.	0.8	5
281	Dy2Cu2O5 nanostructures: Sonochemical fabrication, characterization, and investigation of photocatalytic ability for elimination of organic contaminants. Journal of Molecular Liquids, 2021, 344, 117883.	2.3	5
282	Synthesis of La9.33Si6O26 nano-photocatalysts by ultrasonically accelerated method for comparing water treatment efficiency with changing conditions. Arabian Journal of Chemistry, 2022, 15, 103481.	2.3	5
283	Eco-friendly sonochemistry preparation and electrochemical hydrogen storage of LaCoO3/CoO/La2O3 nanocomposites. Fuel, 2022, 311, 122544.	3.4	5
284	Efficient purification of wastewater by applying mechanical force and BaCO <sub>3</sub> /TiO <sub>2</sub> and BaTiO <sub>3</sub> /TiO <sub>2</sub> piezocatalysts. RSC Advances, 2021, 11, 37138-37149.	1.7	5
285	Agaricus bisporus extract as an excellent biotemplate agent for the synthesis of nano-plate Dy2Ti2O7/g-C3N4 and its application in electrochemical hydrogen storage. Fuel, 2022, 317, 123475.	3.4	5
286	Synthesis, characterization and catalytic oxidation of tetrahydrofuran with 16-membered pentaazabis(macrocyclic) copper(II) complexes; {[Cu([16]aneN5)]2R}4+ (RÂ=Âaromatic nitrogen–nitrogen) Tj	E1@q00(	) <b>r</b> gBT /Over
287	Synthesis and Characterization of AgSCN Micro/Nanostructures by Sonochemical Method. Synthesis and Reactivity in Inorganic, Metal Organic, and Nano Metal Chemistry, 2015, 45, 1191-1198.	0.6	4

Graphite Nanosheets: Thermal Treatment Synthesis and Characterization. Synthesis and Reactivity in Inorganic, Metal Organic, and Nano Metal Chemistry, 2016, 46, 877-882.

#	Article	IF	CITATIONS
289	Synthesis of SiO2 Nanocrystals by Two Approaches and Their Application in Photocatalytic Degradation and Flame Retardant Polymeric Nanocomposite. Journal of Inorganic and Organometallic Polymers and Materials, 2019, 29, 378-389.	1.9	4
290	Sol–gel auto combustion synthesis, characterization, and application of Tb <sub>2</sub> FeMnO <sub>6</sub> nanostructures as an effective photocatalyst for the discoloration of organic dye contaminants in wastewater. RSC Advances, 2021, 11, 26844-26854.	1.7	4
291	Facile sonochemical method for preparation of Cs2Hgl4 nanostructures as a promising visible-light photocatalyst. Ultrasonics Sonochemistry, 2021, 80, 105827.	3.8	4
292	Electrochemical hydrogen storage capacities of sol-gel synthesized Dy3Fe5O12/DyFeO3 nanocomposites: Schiff-base ligand-assisted synthesis and characterization. Fuel, 2022, 324, 124600.	3.4	4
293	Facile sonochemical preparation of La2Cu2O5 nanostructures, characterization, the evaluation of performance, mechanism, and kinetics of photocatalytic reactions for the removal of toxic Synthesisand Characterization of Cooper(11)2Complex Nanoparticles	2.3	4
294	([Cu([18]py} <sub>2</sub> N <sub>4</sub> )] <sup>2 +</sup> ,) Tj ETQq0 0 0 rgBT /Overlock 10 Tf 50 557 Td ([Ci	0.6	<sub>2</sub>
295	Zeolite-Y. Synthesis and Reactivity in Inorganic, Metal Organic, and Nano Metal Chemistry, 2010, 40, INVESTIGATION OF ADSORPTION AND INHIBITIVE PROPERTIES OF SOME DIAMINE COMPOUNDS ON MILD STEEL CORROSION IN HYDROCHLORIC ACID SOLUTION. Chemical Engineering Communications, 2014, 201, 1077-1095.	1.5	3
296	Simple Thermal Decompose Method for Synthesis of Nickel Disulfide Nanostructures. High Temperature Materials and Processes, 2016, 35, 1017-1019.	0.6	3
297	Synthesis and Characterization of Mg(OH) <sub>2</sub> and MgO Nanostructures Via Simple Hydrothermal Method. Synthesis and Reactivity in Inorganic, Metal Organic, and Nano Metal Chemistry, 2016, 46, 681-686.	0.6	3
298	Toxicity of Nd <sub>2</sub> WO <sub>6</sub> nanoparticles to the microalga <i>Dunaliella salina</i> : synthesis of nanoparticles and investigation of their impact on microalgae. RSC Advances, 2021, 11, 27283-27291.	1.7	3
299	Toxicity evaluation and preparation of CoWO4 nanoparticles towards microalga Dunaliella salina. Environmental Science and Pollution Research, 2021, 28, 36314-36325.	2.7	3
300	Sonochemical synthesis and characterization of Cu2Hgl4 nanostructures photocatalyst with enhanced visible light photocatalytic ability. Arabian Journal of Chemistry, 2022, 15, 103536.	2.3	3
301	Eco-friendly synthesis by Rosemary extract and characterization of Fe3O4@SiO2 magnetic nanocomposite as a potential adsorbent for enhanced arsenic removal from aqueous solution: isotherm and kinetic studies. Biomass Conversion and Biorefinery, 2024, 14, 5109-5123.	2.9	3
302	Effects of the NiFe <sub>2</sub> O <sub>4</sub> nanoadditive on the performance and emission characteristics of diesel engines: ultrasonic green synthesis by T3 hormone. RSC Advances, 2021, 11, 27701-27713.	1.7	2
303	Green self-assembly of CuCe2(MoO4)4/montmorillonite-K10 nanocomposites; a promising solid-state hydrogen storage profile. Fuel, 2022, 310, 122401.	3.4	2
304	Synthesis and Characterization of Nickel(II) Complexes with 18-Membered Decaaza Macrocycles 1,10-dialkyl-5,6,14,15-tetraphenyl-1,3,4,7,8,10,12,13,16,17-decaazacyclooctadecane. Synthesis and Reactivity in Inorganic, Metal Organic, and Nano Metal Chemistry, 2005, 35, 469-475.	0.6	1
305	Solvothermal Synthesis and Characterization of PbSe Nanostructures with the Aid of Schiff-base Ligand. Journal of Cluster Science, 2013, 24, 657-667.	1.7	1
306	Green sonochemistry fabrication of pure Gd2Sn2O7 nanoparticles with advanced photocatalytic efficiency for elimination of dye pollutions. International Journal of Hydrogen Energy, 2022, 47, 5269-5280.	3.8	1

#	Article	IF	CITATIONS
307	A simple hydrothermal route for the preparation of novel Na–Y–W nano-oxides and their application in dye degradation. RSC Advances, 2022, 12, 4913-4923.	1.7	1
308	Auto-combustion synthesis of Sr2Fe2O5/Dy3Fe5O12 nanocomposite using Hordeum vulgare L extract: Preparation, structural analysis and evaluation of its photocatalytic and electrochemical behaviors. Journal of Alloys and Compounds, 2022, 896, 163032.	2.8	0